Light-Scattering Characteristics Of Optical Surfaces

James Harvey

James E. Harvey, "Light-Scattering Characteristics Of Optical Surfaces," Proc. SPIE 0107, Stray Light Problems in Optical Systems, (26 September 1977); doi: 10.1117/12.964594

Event: 1977 SPIE/SPSE Technical Symposium East, 1977, Reston, United States

LIGHT-SCATTERING CHARACTERISTICS OF OPTICAL SURFACES

James E. Harvey
Optical Sciences Center
The University of Arizona
Tucson, Arizona 85721

Abstract

A scalar theory of surface scattering phenomena has been formulated by utilizing the same Fourier techniques that have proven so successful in the area of image formation. An analytical expression has been obtained for a surface transfer function which relates the surface micro-roughness to the scattered distribution of radiation from that surface. The existence of such a transfer function implies a shift-invariant scattering function which does not change shape with the angle of the incident beam. This is a rather significant development which has profound implications regarding the quantity of data required to completely characterize the scattering properties of a surface. This theory also provides a straightforward solution to the inverse scattering problem (i.e., determining surface characteristics from scattered light measurements) and results in a simple method of predicting the wave length dependence of the scattered light distribution. Both theoretical and experimental results will be presented along with a discussion of the capabilities and limitations of this treatment of surface scatter phenomena.

Introduction

The relationship between surface micro-roughness and radiant energy scattering plays an important role in many areas of technical interest. These include the cost versus performance trade-offs in the fabrication of optical surfaces, design considerations for stray light rejection systems, evaluation of machined metal mirrors for high energy laser applications, laser radar backscatter signature programs, and a host of other applications requiring extensive scattering data.

The work reported here is an attempt to provide further insight into the scattering process. A scalar theory of surface scatter phenomena has been formulated by utilizing the same Fourier techniques that have proven so successful in the area of image formation. An analytical expression has been obtained for a surface transfer function which relates the surface micro-roughness to the scattered distribution of radiation from that surface. For a large class of well-behaved surfaces it is possible to describe this transfer function in terms of only the rms surface roughness and the surface auto-covariance function. This theory provides a straightforward solution to the inverse scattering problem (i.e., determining the relevant surface characteristics from scattered light measurements). Once the surface characteristics are known, the same theory provides an equally simple method of predicting the wavelength dependence of the scattered light distribution. Furthermore, the mere existence of such a transfer function implies a shift-invariant scattering function which does not change shape with the angle of the incident beam. This is a rather significant development which has profound implifications regarding the quantity of data required to completely characterize the scattering properties of a surface.

Experimental verification of the shift-invariant scattering function and the associated solution to the inverse scattering problem has been successfully demonstrated for smooth surfaces ($\sigma \ll \lambda$), and the predictions of the scattering behavior as a function of wavelength have been shown to be accurate for wavelength changes over a limited spectral range. The light scattering properties of rough (diffusely reflecting) optical surfaces do not exhibit the shift-invariant behavior predicted by the simple theory. However, a more general theoretical treatment results in an infinite family of transfer functions which are required to completely characterize the scattering properties of a rough surface. The results of experimental measurements on several baffle materials exhibiting wide variations in scattered light behavior are presented and discussed in the context of these theoretical developments.

Scattered Light Measurements

Scattered light data is usually collected on an observation hemisphere with some type of goniometric instrument. Figure 1 shows the incident beam striking the scattering surface at some angle of incidence, a specularly-reflected beam striking the observation hemisphere at the position indicated, and the scattered light distribution being sampled at an arbitrary point on the hemisphere.

It is well known that the scattered light distribution on the hemisphere will, in general, change shape drastically with angle of incidence--becoming quite skewed and asymmetrical at large angles of incidence. However, DeBell and Harvey[1] showed that for certain surfaces with well-behaved statistics, if the data collected on the hemisphere is divided by the cosine of the observation angle then plotted as a function of the direction cosines of the observation point, a new scattering function is obtained which will not change shape but will merely be shifted in direction cosine space with changes in angle of incidence. This is a rather significant development which has profound implications regarding the quantity of data required to completely characterize a scattering surface.

Please note that β is the direction cosine of the position vector of the observation point and β_o is the direction cosine of the position vector of the specularly-reflected beam. These direction cosines are obtained by merely projecting the respective points on the hemisphere back onto the plane of the sample and normalizing to a unit radius.

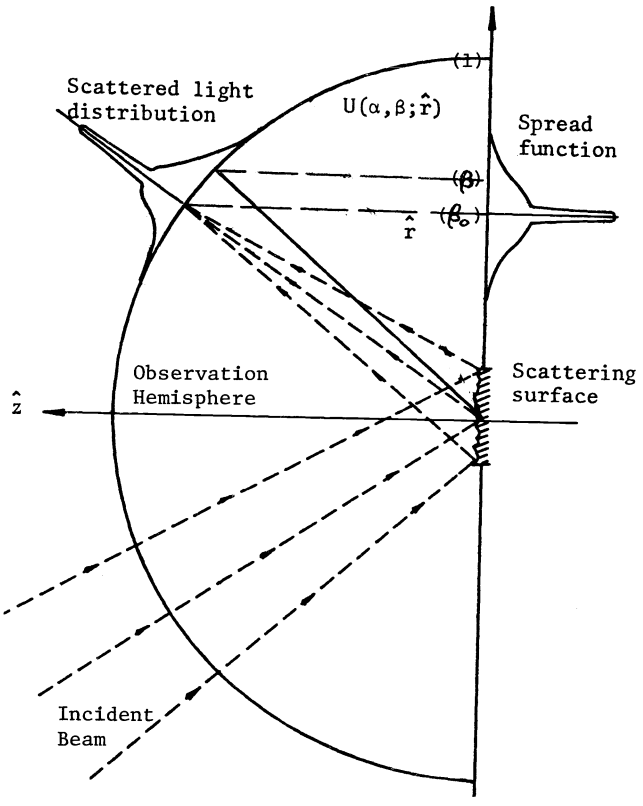

Fig. 1. Geometrical relationship between incident beam, scattering surface, the scattered light distribution, and the resulting spread function.

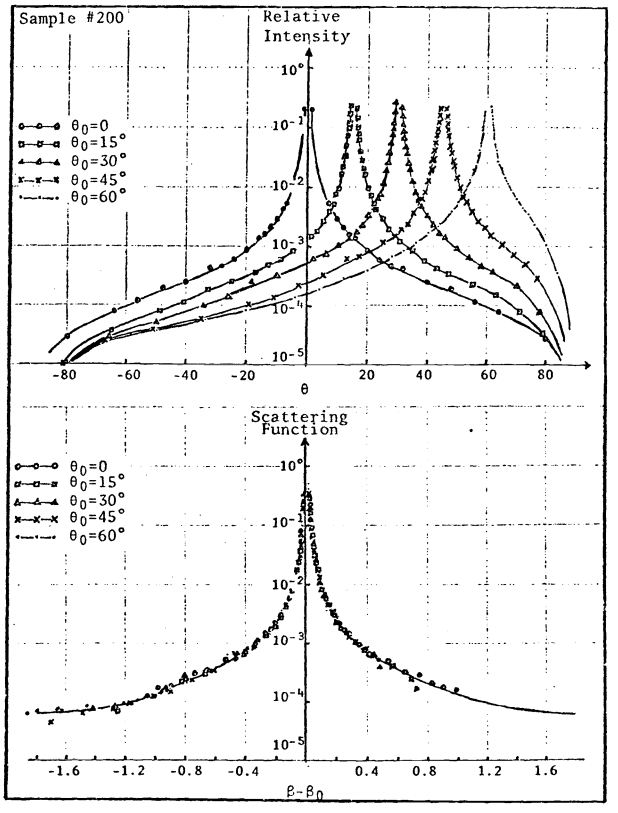

Fig. 2. Illustration of shift-invariance in direction cosine space.

At the top of Figure 2 experimental scattering data from an aluminized quartz mirror is displayed in the usual way by plotting scattered intensity v.s. the observation angle for several different angles of incidence. And we observe the expected asymmetry for large angles of incidence. At the bottom of the figure the same data has been divided by the cosine of the observation angle and plotted as a function of $\beta - \beta_o$, which is the distance of the observation point from the specular beam in direction cosine space. As you can see, the five curves with the incident angle varying from zero to 60^o coincide almost perfectly. The data on this slide confirms that for a certain class of surfaces the scattering properties of the surface are indeed shift-invariant, and can be completely characterized by a single set of measurements at a fixed angle of incidence (i.e. the four-dimensional BRDF degenerates into a single rotationally symmetric two-dimensional scattering function). This shift-invariant behavior implies the existence of a surface transfer function which completely characterizes the scattering properties of the surface.

The Surface Transfer Function

Figure 3 illustrates the surface height, W, as a function of distance along the surface. This surface profile has associated with it an autocovariance function and a surface height distribution function.

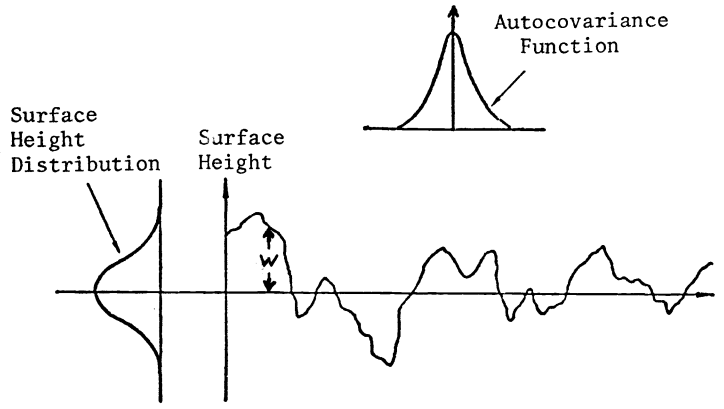

Fig. 3. Illustration of Surface Height Variations and Associated Statistical Parameters.

By describing surface scatter phenomena as a diffraction process in which the rough surface introduces random phase variations into the effective pupil function of the system, an analytical expression can be obtained for the transfer function of the scattering surface.[2] If we assume a stationary process (i.e., a random, homogeneous, isotropic mirror surface), and a gaussian surface height distribution function, this transfer function is described only in terms of the rms surface roughness and the surface autocavariance funtion

$$\mathcal{H}(\hat{x},\hat{y}) = e^{-(4\pi\hat{\sigma})^2\left[1 - \frac{C(\hat{x},\hat{y})}{\hat{\sigma}^2}\right]} \qquad 1.)$$

where

$$\hat{x} = x/\lambda \quad \hat{y} = y/\lambda \ , \quad \hat{\sigma} = \sigma/\lambda. \qquad 2.)$$

Considerable insight into the scattering process can now be obtained by considering the nature of this transfer function. The autocovariance function approaches the value σ^2 as the displacement approaches zero. The equivalent transfer function thus approaches unity as expected. As the displacement approaches infinity the autocovariance function approaches zero and the equivalent transfer function approaches a plateau of height $\exp\left[-(4\pi\hat{\sigma})^2\right]$. This behavior is illustrated in Fig. 4.

The equivalent transfer function of the scattering surface can thus be regarded as the sum of a constant component and a bell-shaped component and can therefore be rewritten as

$$\mathcal{H}(\hat{x},\hat{y}) = A + B\,Q(\hat{x},\hat{y})$$

$$A = e^{-(4\pi\hat{\sigma})^2}$$

$$B = 1 - e^{-(4\pi\hat{\sigma})^2}$$

$$Q(\hat{x},\hat{y}) = \frac{e^{(4\pi\hat{\sigma})^2\,\frac{C(\hat{x},\hat{y})}{\hat{\sigma}^2}} - 1}{e^{(4\pi\hat{\sigma})^2} - 1}$$

The significance of this interpretation of the transfer function is shown by the inferred properties of the corresponding spread function. Since the transfer function is the sum of two separate components, the equivalent spread function of the scattering surface is the sum of the inverse Fourier transforms of the two component functions. The constant component transforms into a delta function, and the bell-shaped component transforms into a bell-shaped scattering function as shown in Figure 5. Hence the scattering surface reflects an incident beam of light as a specularly-reflected beam of diminsihed intensity surrounded by a halo of scattered light. Furthermore, the relative power distribution between the specular component and the scattered component of the effective spread function are given by the quantities A and B, respectively.

By describing the transfer function in terms of the normalized spatial variables, the reciprocal variables in Fourier transform space are the direction cosines of the propagation vectors as suggested by our previous disucssion of a shift-invariant scattering function in direction cosine space.

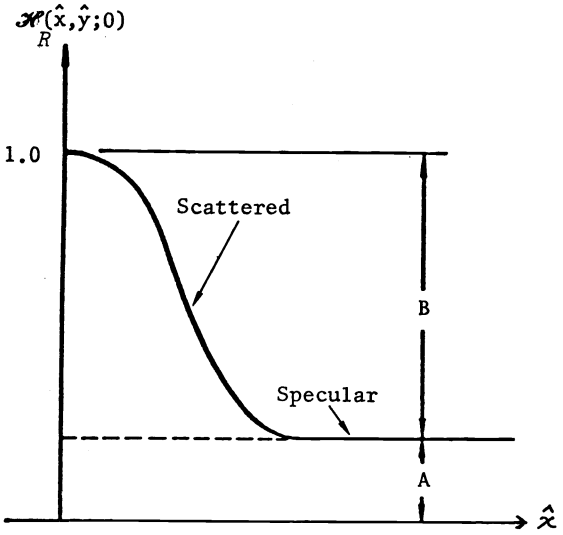

Fig. 4. Effective transfer function of a scattering surface.

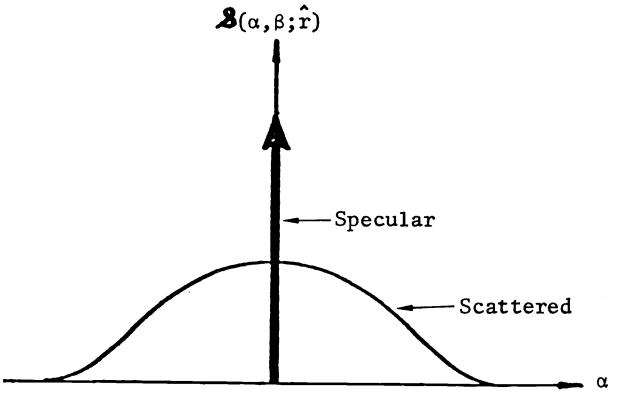

Fig. 5. Spread function associated with a scattering surface.

The Inverse Scattering Problem

A computer program has been developed for calculating the effective transfer function and the surface autocovariance function from scattered light data as shown in Figure 6. The measured data are assumed to be a radial profile, $S(\rho)$, of a rotationally-symmetric scattering function. An intermediate quantity, $BQ(\hat{s})$, is first determined by calculating the two-dimensional Fourier-Bessel Transform of this scattering function. The surface transfer function is then calculated using Eq.3.), and finally, the surface autocovariance function is computed from Eq.1.). Note that the Total Integrated Scatter, B, and the rms surface roughness, σ, are also provided by this technique.

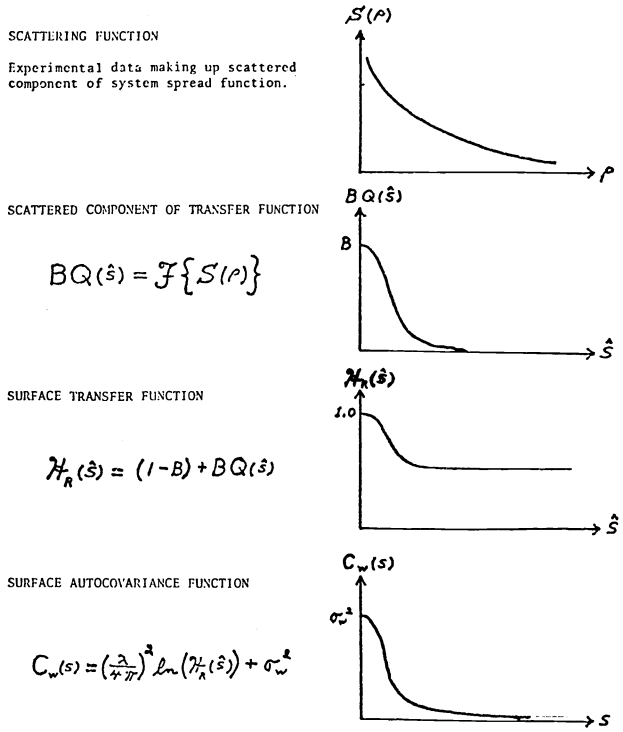

Fig. 6. Outline of inverse scattering program.

Fig. 7 illustrates the predicted surface autocovariance function for a typical mirror surface. Faborable comparisons of predicted surface characteristics with independant measurements made at the Naval Weapons Center in China Lake, California have been demonstrated for several different mirror surfaces. In additon, experimental verification of the inverse scattering program was indirectly accomplished by supplying scattered light data of one wavelength as input to the inverse scattering program in order to determine the relevant surface characteristics; then this information was used to predict the scattering function at a different wavelength. Excellent agreement with the measured scattering function at that wave-length was achieved as indicated in Figure 8.

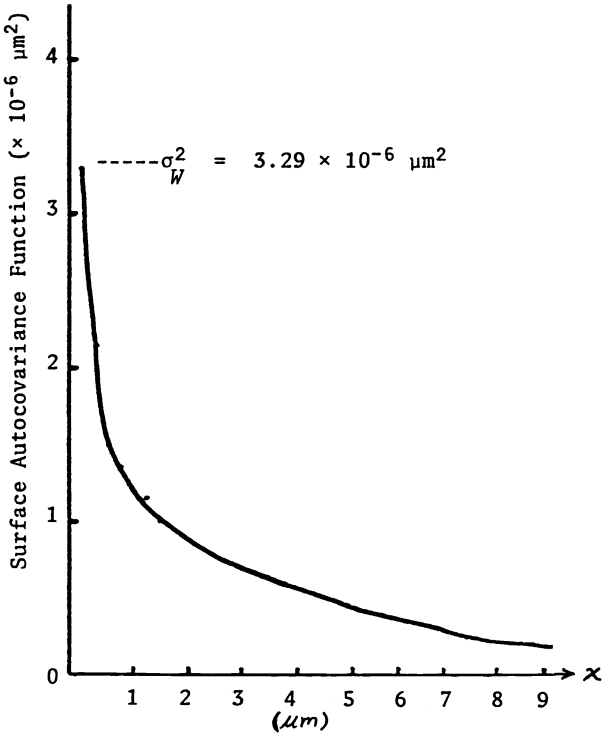

Fig. 7. Surface Autocovariance Function for Sample #198 Prediced from Scattered Light Measurements at λ = 0.5145 um.

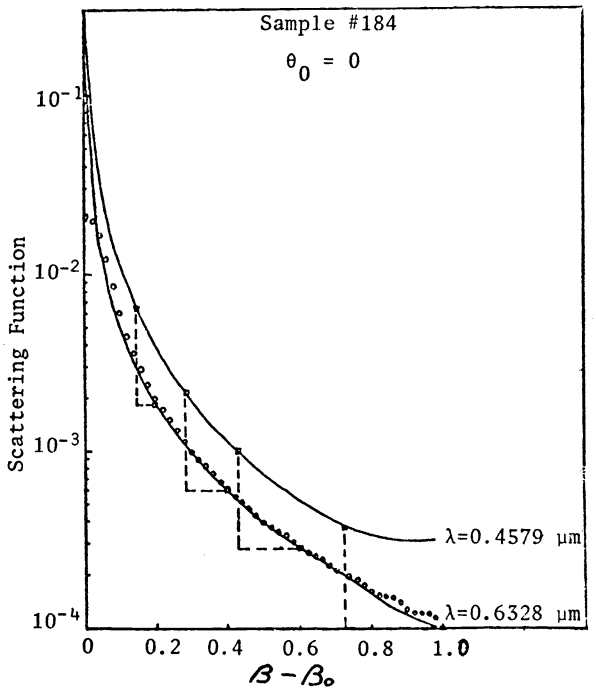

Fig. 8. Indirect verification of the inverse scattering problem.

The Wavelength Dependence of the Scattered Light Distribution

The above technique for predicting the scattering behavior of a surface at some wavelength from measured data at a different wavelength involves only numerical computations on sampled data. An analytical expression for a wavelength scaling law is therefore not required to determine the scattering function at any desired wavelength. However, in order to gain insight into the wavelength dependence of surface scatter phenomena, the following wavelength scaling law for smooth surfaces was derived:

$$S(\alpha, \beta; a\lambda) = \frac{1}{a^4} S(\alpha/a, \beta/a; \lambda). \qquad 7.)$$

Note that, in addition to the $1/a^4$ change in magnitude, the width of the scattering function in direction cosine space is scaled by the factor a. This behavior is verified by the dashed lines in Fig. 8. An attempt to predict the scattering function at 10.6 μm from measured data in the visible was not successful. This failure was due to the greatly expanded angular width of the scattering function at long wavelengths in accordance with the wavelength scaling law expressed in Eq. 7. For large changes in wavelength this angular shift can extend beyond the angular range over which one has measurement capability. For example, Fig. 9 illustrates that scattered light measurements over angular range from 1^o to 46^o at a wavelength of 0.4579 um can be used to predict the scattering behavior from 1.4^o to 90^o for a wavelength of 0.6328 um. However, these same measurements provide only a few data points in the angular range from 1^o to 2.5^o that are useful in predicting the scattering behavior for a wavelength of 10.6 um, and no information is obtained concerning the scattered light behavior at angles less than 24^o.

It is now clear that it may not be possible to compare the scattered intensity of two widely separated wavelengths in a given direction without extrapolating one curve. However, this behavior has the advantage of allowing one to determine the scattering characteristics at very small angles (unobtainable by direct measurement due to mechanical constraints) by making large angle scatter measurements at a longer wavelength.

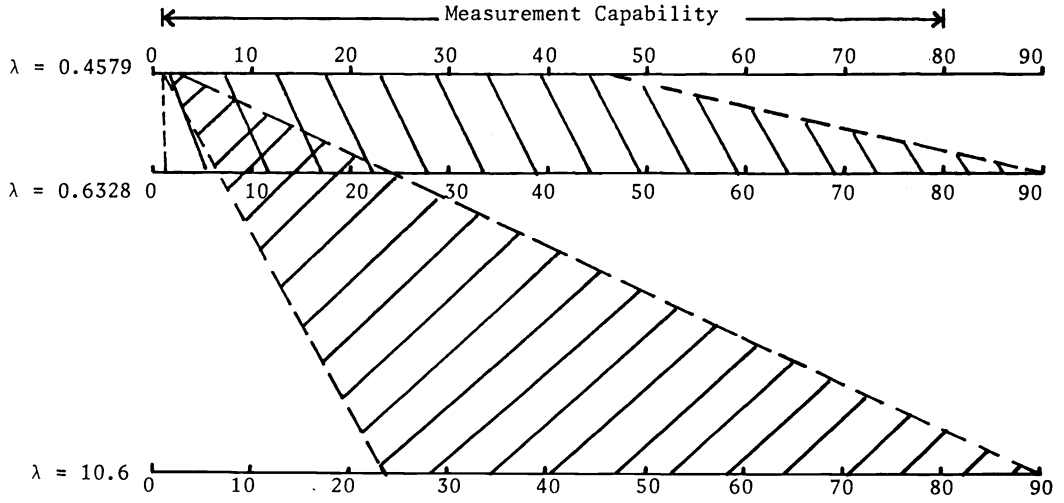

Fig. 9. Diagram Illustrating the Effects of the Wavelength Scaling Law.

Discussion

This study has been a general investigation of surface scatter phenomena dealing with several different aspects of scattered light behavior. An elementary theoretical development based upon scalar diffraction theory has been presented. Linear systems theory and modern Fourier techniques result in a theoretical model of light scattering systems which closely parallels the highly successful theory of isoplanatic imaging systems. An extensive experimental program has successfully verified this theoretical development for a certain class of well-behaved surfaces.

However, most baffle surfaces of interest do not obey this simple theoretical model. Fig. 10 and Fig. 11 illustrate the scattering behavior exhibited by two such surfaces.

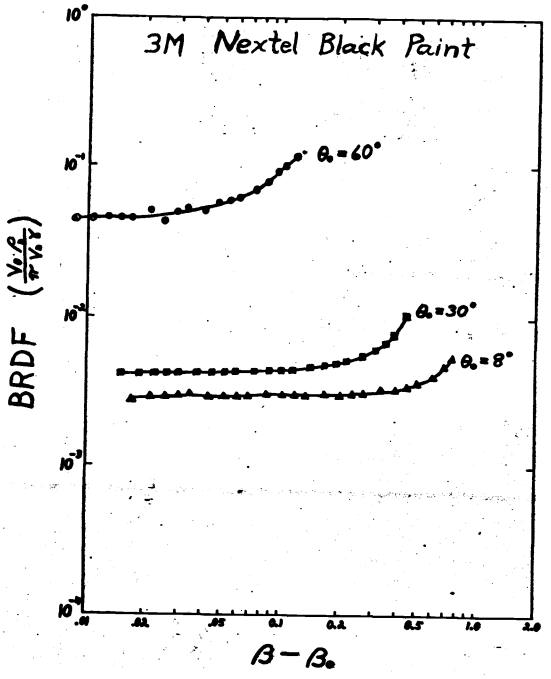

Fig. 10. BRDF Measurement at 10.6μm.

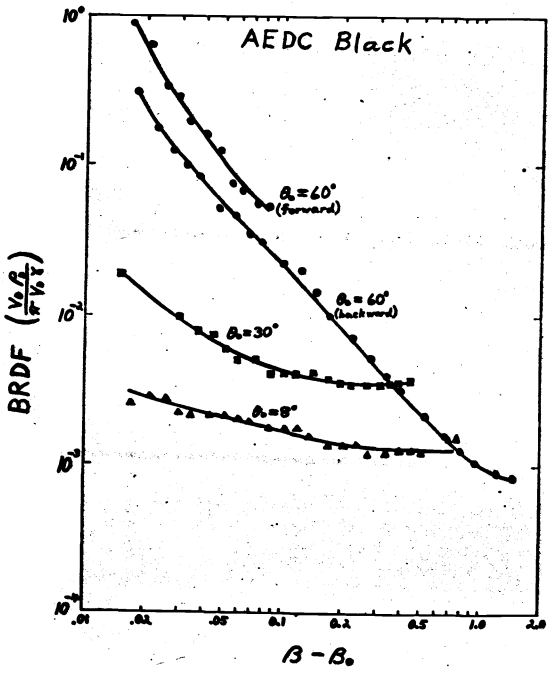

Fig. 11. BRDF Measurements at 10.6μm.

No explicit approximations concerning the size of the surface variations were made in the theoretical development discussed here. However, a simplifying assumption was made regarding the random component of the pupil function. It was assumed that the phase variations in the disturbance emerging from the scattering surface were equal to the perturbations introduced onto a normally incident wavefront. Careful examination of Fig. 12 reveals that the phase difference introduced by reflection from a rough surface depends upon both the angle of incidence and the angle of observation in addition to the surface height at the point of relfection. The phase variations along the scattering surface can thus be expressed as

$$\phi(x,y) = 2\pi(\gamma+\gamma_o)\,W \qquad 8.)$$

where

$$\gamma = \cos\theta, \quad \gamma_o = \cos\theta_o. \qquad 9.)$$

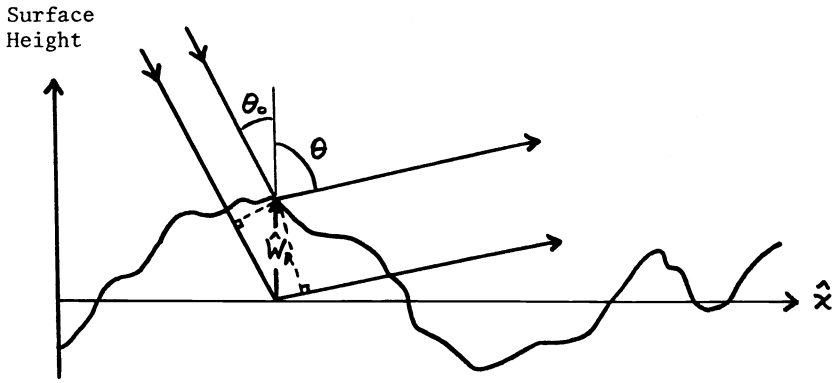

Fig. 12. Illustration of the Phase variation introduced by reflection from a rough surface.

The effective transfer function of a scattering surface is now given by the following general expression

$$\mathcal{H}(\hat{x},\hat{y}) = e^{-[2\pi(\gamma+\gamma_o)\hat{\sigma}]^2\left[1-\frac{C(\hat{x},\hat{y})}{\hat{\sigma}^2}\right]} \qquad 10.)$$

This expression can be interpreted as a two-parameter family of tranfer functions, one for every possible angle of incidence and every possible scattering angle.

This generalization still leaves us with a theoretical model which closely parallels that of non-isoplanatic imaging systems which can be characterized by a different transfer function for each off-axis object point.

References

1. DeBell, M. A. and J. E. Harvey, "Recent Developments in Surface Scatter Studies," Abstract, J. Opt. Soc. Am. 64:1404 (1974).

2. Shack, R.V. and J. E. Harvey, "An Investiagation of the Relationship between Surface Microroughness and Radiant Energy Scattering", Final Report, SAMSO Contract No. 404701-75-C-0106. (1976).